Electrochimica Acta 135 (2014) 42–51

Contents lists available at ScienceDirect

Electrochimica Acta

journal homepage: www.elsevier.com/locate/electacta

Application of the combined electrochemical quartz crystal microbalance and probe beam deflection technique in deep eutectic solvents

A. Robert Hillman[a,*], Karl S. Ryder[a], Christopher J. Zaleski[a], Virginia Ferreira[a], Christopher A. Beasley[b], Eric Vieil[c]

[a] Department of Chemistry, University of Leicester, Leicester LE1 7RH, UK
[b] Gamry Instruments, Warminster, PA, 18974, USA
[c] LEPMI, UMR 5279, CNRS, Université de Grenoble, F-38402 Saint Martin d'Hères, France

ARTICLE INFO

Article history:
Received 21 December 2013
Received in revised form 10 April 2014
Accepted 12 April 2014
Available online 2 May 2014

Keywords:
Probe beam deflection
quartz crystal microbalance
deep eutectic solvent
electrocrystallization
silver
tin

ABSTRACT

The electrochemical quartz crystal microbalance (EQCM) and probe beam deflection (PBD) have been widely used to study interfacial processes in molecular solvent-based electrolytes. However, there has been limited use of the EQCM and none of PBD in room temperature ionic liquids, including deep eutectic solvents (DES). Here we explore the use of the combined EQCM/PBD technique to the study of Ag and Sn electrodeposition from a DES comprising a 1:2 mixture of choline chloride and ethylene glycol. While overcoming the effect of viscous loss in the acoustic wave (EQCM) part of the experiment is understood, the optical (PBD) technique fails to provide a meaningful response in slow scan rate voltammetric experiments; this contrasts sharply with the straightforward behaviour seen in aqueous media. Solution transport considerations reveal this to be a consequence of long surface-to-beam transit times in the viscous DES. The problem can be overcome by operating at scan rates 1-2 orders of magnitude slower, permitting application of this powerful technique to novel media of technological interest. The PBD responses reveal unanticipated chemical effects: multiple complexes in the Ag system and solubility limitations in the Sn system, neither of which is evident from the electrochemical or QCM responses.

1. Introduction

The electrochemical quartz crystal microbalance (EQCM) [1–3] and probe beam deflection (PBD) [4–6] techniques have individually proved to be extremely useful probes of interfacial processes that involve exchange of chemical species between an electrode surface and its ambient electrolyte solution. These encompass such diverse processes as electropolymerization [7–11], electrocrystallization [12], adsorption [13,14], absorption [15], underpotential deposition (UPD) [16,17] and electroactive film redox switching [8,18–25]. Since the EQCM, in the simplest and most commonly used mode, is a gravimetric probe, it is sensitive to the transfer of neutral species (notably solvent) and has high sensitivity to the deposition and dissolution of heavy species, notably metals. However, it is predictably less sensitive to light species: the extreme case is the transfer of protons to/from an electroactive film in order to maintain electroneutrality [26]. The physical basis of the PBD technique is associated with a gradient of refractive index, so its sensitivities to various species are quite different to that of the EQCM; for example, interfacial proton transfers may be detected readily [27] but solvent transfer much less so.

It is quite clear from the above considerations that a combination of the EQCM and PBD techniques promises considerable power and sensitivity. Strictly, since the electrochemical and acoustic ("E" and "QCM") measurements are separate, there are three measurands in a typical EQCM/PBD experiment: current (or charge), mass and optical deflection. Consequently, by combining the outputs of the three simultaneous experiments, this holds the promise of resolving the transfers of up to three species, for example the anion and cation of the electrolyte and solvent [28,29]. That this is the case has been demonstrated for metal electrodeposition under UPD [30] or bulk [31] conditions and electroactive polymer film redox switching [32].

Interestingly, all the above studies used conventional electrolytes, based on molecular solvents typified by water or acetonitrile. Recently, there has been considerable interest in the

* Corresponding author.
E-mail address: arh7@le.ac.uk (A.R. Hillman).

http://dx.doi.org/10.1016/j.electacta.2014.04.062
0013-4686/

use of a range of room temperature ionic liquids (RTIL) [33] and deep eutectic solvents (DES), for example based on quaternary ammonium salts (QAS) and hydrogen bond donors (HBD) [34,35]. Interest in the use of these novel media is provoked by both practical and fundamental aspects. In the former instance, they offer very high ionic concentrations (e.g. high ion availability for charge storage applications), wide potential windows, excellent solvating power for a wide range of electroactive species and low environmental impact. These attributes have generated considerable attention in the literature for applications involving metal plating and related electrodeposition processes, where they provide practical alternatives for aqueous-based formulations that involve toxic or otherwise environmentally unacceptable components [36].

In the latter instance, the notion of a medium that is exclusively ionic (at ambient conditions) is extremely interesting. In the context of electroactive polymer films, molecular solvents have been shown to play a major role in controlling viscoelastic properties and thence film mechanical behaviour and ion transport rates. Consequently, the removal of such species from the system suggests that interesting and novel effects might be observed.

These ideas motivate the use of the EQCM/PBD technique to study electrochemical processes involving RTIL and DES media. Based on the phenomena underlying the QCM and PBD techniques, accomplishing this will require consideration of the *physical* (*cf. chemical*, above) characteristics of these media. Specifically, the very high viscosities of some RTIL/DES systems (1-3 orders of magnitude greater than water or typical organic solvents) may be expected to increase damping (energy dissipation) of the QCM crystal resonance and to diminish the fluxes of species to/from the interface. From the perspective of PBD, the notion of local changes in "electrolyte concentration" ceases to have the same physical meaning and some simple considerations of molar refractivity of the components suggests that the refractive index gradients (and thence optical deflections) may be smaller.

There are clearly significant opportunities but also substantive challenges in the application of the EQCM/PBD methodology to interfacial processes involving RTIL and DES media. The generic goals of the present study are to identify which of the challenges identified above is predominant and, *via* appropriate instrumental and analytical interventions, to resolve them in order that the combined EQCM/PBD technique can be implemented in these fundamentally and technologically interesting media. While there are a few reports of the EQCM being used to study electrochemical processes in RTILs, these are predominantly the less practicable imidazolium-based [37,38] or pyrrolidinium-based [37,39,40] systems and there are few studies in DES media [41,42]. To the best of our knowledge, neither the PBD technique nor the combined EQCM/PBD technique has been used to study interfacial processes in RTILs or DESs. The generic aim of this work is to overcome the practical measurement challenges presented by these systems. As we shall show, this creates the opportunity for novel fundamental studies of practical significance in electrochemically controlled aspects of energy storage, materials science, corrosion protection and metal finishing.

2. Experimental

2.1. Materials

$AgNO_3$, AgCl, $SnCl_2$, choline chloride and ethylene glycol (Sigma Aldrich) were used as received. The DES was formed by mixing the QAS (choline chloride, which we represent as Ch^+Cl^-) with the HBD (ethylene glycol, which we represent as EG) in a 1:2 molar ratio. We will use the shorthand notation $Ch^+Cl^-(EG)_2$ for this formulation. (Note: it is sometimes referred to as *Ethaline 200* [41]; the number denotes the stoichiometry which, in this instance, results in complexation of the anion by the ethylene glycol such that there are no free neutral molecules.)

2.2. Instrumentation

The electrochemical cell comprised a standard three-electrode configuration mounted inside an optical glass cuvette (Hellma, 42 × 42 × 30 mm). A 10 MHz AT–cut Au plated quartz crystal working electrode (ICM Manufacturing, Oklahoma City, USA, piezoactive area 0.21 cm^2), was mounted on the end of a glass tube. The counter electrode was an Ir-coated Ti mesh (area 5.50 cm^2). An Ag/AgCl wire exposed to the chloride-containing DES medium was used as a reference electrode; this has previously been shown to provide a stable reference potential in choline chloride-based eutectics [43].

The electrochemical, gravimetric and optical signals were recorded simultaneously using a Gamry Reference 600 potentiostat integrated with Gamry eQCM 10 M micro-gravimeter. The potentiostat was coupled to a home-built optical deflection system based on that described previously [31]. The optical deflection measurements were conducted using a dual photodiode which was set 18.5 cm from the electrochemical cell, resulting in a position sensitivity of 0.44 μrad/mV.

2.3. Procedures

Silver was deposited/dissolved potentiodynamically by cycling the applied potential between 0.2 and -0.3 V at potential scan rates in the range 2.5 - 10 mV s^{-1} in aqueous electrolyte (0.001 M $AgNO_3$/0.2 M $HClO_4$) and 0.0625–0.5 mV s^{-1} in $Ch^+Cl^-(EG)_2$ (containing 0.01 M AgCl). A similar procedure was used for the tin system (0.01 M $SnCl_2$ in $Ch^+Cl^-(EG)_2$), but with potential limits of -0.34 and -0.68 V and scan rates in the range 0.03125–0.25 mV s^{-1}. All measurements were made at room temperature (20 ± 2 °C).

2.4. Data analysis

Interpretation of the QCM frequency response took into account two factors. First, the solution is purely viscous; there is no storage component to the complex modulus. Second, the similar values of the resonant admittance for bare and for polymer-coated electrodes immersed in the DES demonstrate that there is no significant viscous loss associated with the film, i.e. the loss modulus is much less than the storage modulus. Thus, the films of the thickness used here are acoustically thin (in common parlance "rigid", although this is not accurate use of the terminology [1],[3]). Consequently, the frequency response can be interpreted in gravimetric terms using the Sauerbrey equation [44]. This is the case for both the Ag and Sn systems. Additionally "calibration" data for Ag deposition are provided *via* the mass-charge relationship in both integral (Δm-Q) and differential (δ(Δm)/δt-i) variants.

The angular deflection (θ) of the laser beam by the interfacial concentration gradient perpendicular to the surface, $\delta c(x,t)/\delta x$, is described by:

$$\theta(x,t) = \left(\left(\frac{1}{n}\frac{\delta n}{\delta c}\right)\left(\frac{\delta c(x,t)}{\delta x}\right)\right) \quad (1)$$

where l is the interaction length of the light beam with the surface (here, the electrode diameter), x is the distance of the laser beam from the electrode surface and ($\delta n/\delta c$) represents the variation of refractive index (n) with concentration (c). The laser beam is deflected toward the region of higher refractive index. The instrument was set up such that a positive (negative) deflection represents decreasing (increasing) refractive index at the surface

of the electrode. Under the conditions employed (notably low laser power), negligible thermal gradients are created in the solution.

Quantitative comparison between the parameters recorded at the electrode surface (i, Δm) and the optical deflection (θ) generated at some distance from the surface requires one to account for the delay between these two sets of signals and their diffusional broadening during transport of species between the surface and the probe beam. This was accomplished using the temporal convolution technique which essentially "projects" the current (i) and mass (Δm) signals to the location where the optical deflection (θ) is measured.

In the case of semi-infinite linear diffusion, the flux, $J(x,t)$, at a distance x from the surface of the electrode at a time t is related to its magnitude $J(t)$ at the electrode surface through a convolution operation (*) with a transfer function $F(x, t)$ [45]:

$$J(x,t) = J(t) * F(x,t) \quad \text{where} \quad F(x,t) = \frac{x}{2(\pi Dt)^{1/2}} exp\left(-\frac{x^2}{4Dt}\right) \tag{2}$$

in which D is the diffusion coefficient of the transported species. This operation may be applied to the current and mass signals. Data analysis involves the use of a scaling factor, $x/\sqrt{D}$, which represents the distance of the light beam from the surface; the latter is generally 50-100 μm and is ultimately limited by the radius of the laser focal zone (typically 30-50 μm). The parameter $x/\sqrt{D}$ has to be fitted since, although it is straightforward to control *relative* changes in the position of the laser beam with respect to the surface, precise determination of *absolute* values is difficult; we introduce no new aspect to the procedure for effecting this fitting, which has been described in detail elsewhere [6,31,45].

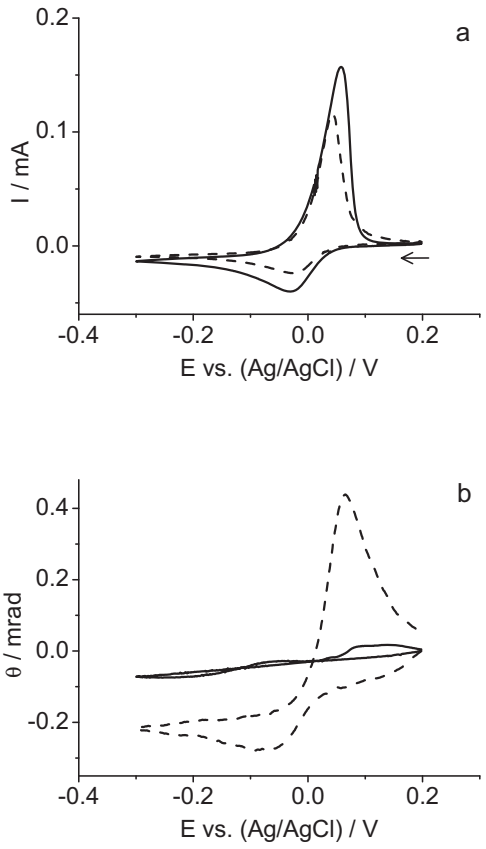

Fig. 1. Deposition of Ag from aqueous (dashed line) and E in $Ch^+Cl^-(EG)_2$ (full line) media. Solution composition: aqueous medium: 0.001 M $AgNO_3$/0.2 M $HClO_4$; DES medium: 0.01 M AgCl/$Ch^+Cl^-(EG)_2$. Panel *a*: *i-E* curves; panel b: *θ-E* curves. Potential scan rate, $\nu = 5$ mV s^{-1}. Potential range 0.2 to -0.3 V; scan initiated from $E = 0.20$ V.

3. Results

3.1. Recognition of the challenge

The challenge of interpreting EQCM/PBD data acquired in DES media can be readily appreciated by comparing the current (i), mass change (Δm) and optical deflection (θ) responses for nominally the same experiment in a typical molecular solvent-based electrolyte and a DES. Fig. 1 shows representative data for two such experiments, involving the notionally straightforward process of silver deposition and dissolution, in one case from aqueous solution and in the other from $Ch^+Cl^-(EG)_2$. Under the conditions employed, the current responses (*i-E* curves in panel *a*) are very similar. Note that this situation is to some extent engineered, in that the lower diffusion coefficient in $Ch^+Cl^-(EG)_2$ (due to the increased viscosity) is compensated by using a higher Ag(I) species concentration. This was deliberately done to explore the surface-to-probe-beam *solution* transport in the two media in the presence of broadly similar *interfacial* fluxes.

In contrast to the current responses, the optical deflection responses (*θ-E* curves in panel *b*) are dramatically different. For this apparently simple electrochemical process, resulting in local depletion of silver ions from the solution in the vicinity of the electrode, one would expect the *θ-E* and *i-E* responses in a given medium to be qualitatively similar due to their dependence on the concentration gradient (see Eq. (1) and consider Fick's laws). This situation is realised in the case of deposition from aqueous medium (dashed lines in Fig. 1), but not in the case of deposition from $Ch^+Cl^-(EG)_2$ (full lines in Fig. 1). In the latter case, the response is also an order of magnitude smaller.

As will become clear with the presentation of other data (see below), this problem is quite general and presents an apparent barrier to the application of the otherwise extremely powerful and informative PBD methodology [5,6]. We now proceed to identify its origin and thereby devise a solution. The primary question is whether the near-absence of response in DES is attributable to the optical detection process *per se* or to other physical attributes of the system.

In the former instance, one has to consider the "contrast" (difference in refractive index) between the components of the system, *i.e.* the electroactive species and the medium. Some straightforward considerations indicate that the magnitude of the response (essentially, refractive index gradient) will be somewhat less in the case of the DES system used. However, this is not beyond the capability of typical instrumentation in this field and in any case this would not change the qualitative shape of the response.

In the latter instance, the most obvious difference between most DES media and typical molecular solvents is their substantially higher viscosity [46]: for the situation shown in Fig. 1, the viscosity of $Ch^+Cl^-(EG)_2$ is *ca.* 40 times that of water. The significance of this is that the PBD is essentially a "downstream" detector and the species generated/consumed at the electrode surface must diffuse to/from the bulk solution. Thus, the time taken for establishment of the concentration gradient (see Eq. (1)) distant from the surface (where the optical beam passes) increases with solvent viscosity. We now explore this in more detail.

Consider diffusional transport of species from the electrode surface to a "downstream" detector positioned a distance h from the electrode/solution interface. In the case of a PBD experiment, this corresponds to the focal zone of the laser beam, with $h \sim 100$ μm. The time (t) taken for this can be approximated using $h \sim \sqrt{(\pi Dt)}$, where D is the diffusion coefficient of the transported species. In aqueous solution, where viscosity $\eta \sim 1$ cP and (for small molecules/ions) $D \sim 5 \times 10^{-6}$ cm^2 s^{-1}, this yields $t \sim$

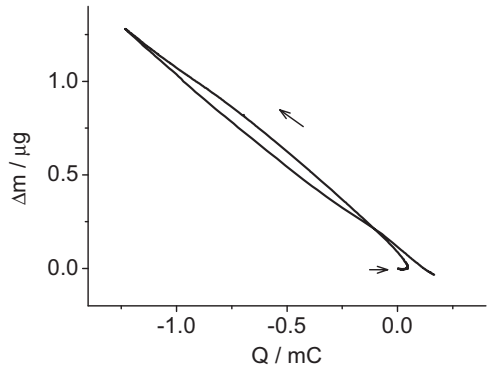

Fig. 2. Deposition of Ag from aqueous medium (0.001 M $AgNO_3$/0.2 M $HClO_4$). Correlation of gravimetric and coulometric responses in integral form: Δm *vs* q. Potential scan rate, ν = 5 mV s^{-1}. Potential range 0.2 to -0.3 V; scan initiated from E = 0.20 V. Arrows indicate scan direction.

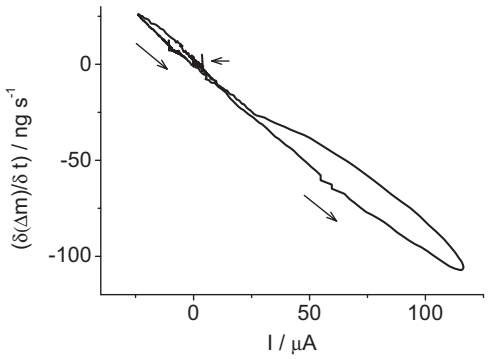

Fig. 3. Deposition of Ag from aqueous medium (0.001 M $AgNO_3$/0.2 M $HClO_4$) (the experiment of Fig. 2). Correlation of gravimetric and coulometric responses in differential form: $\delta(\Delta m)/\delta t$ *vs* i. Potential scan rate, ν = 5 mV s^{-1}. Potential range 0.2 to -0.3 V; scan initiated from E = 0.20 V. Arrows indicate scan direction.

5 s. Viewing the potential axis in the context of a voltammetric experiment (with scan rate ν/mV s^{-1}) as a time axis, this indicates that the optical signal should be "delayed" (i.e. shifted) by an interval vt on the potential axis. In the case of the data in Fig. 1, where ν = 5 mV s^{-1}, this corresponds to a shift of 25 mV. While measureable, this is not dramatic. Turning to the DES, where $\eta \sim 40$ cP, the diffusion coefficient will be proportionately smaller and the diffusion time proportionately longer. For the circumstances of the experiment in Fig. 1, this yields $t \sim 200$ s corresponding to a shift on the potential axis of ca. 1 V. This has three consequences: (i) the half cycle is completed before any product is detected, (ii) by the time the detector "sees" the product, the electrode reaction is proceeding in the opposite direction and (iii) the convolution analysis cannot address the situation of the potential sweep and the detected reaction occurring in opposite senses. In short, the PBD experiment is practically and interpretationally compromised. Resolving this problem is the primary generic goal of the present study.

The foregoing analysis shows that the failure to detect significant reaction in the $Ch^+Cl^-(EG)_2$ experiment of Fig. 1 is attributable to the distant nature of the optical probe. In principle, there are two solutions to the problem: diminution of the distant nature of the optical beam in either space or time. The first of these - translation of the optical beam closer to the surface - is the more obvious choice. However, this is not practical to any useful extent, since the diameter of the focal zone of the laser is on the order of 60 μm and encroachment into this zone would result in scattering of the light beam. The second of these offers greater opportunity by the simple expedient of decreasing the potential scan rate, so the concentration gradients have time to spread out to the laser focal zone within the longer duration of a half cycle. The required decrease in scan rate is on the order of two orders of magnitude, to $\nu \sim 0.05$ mV s^{-1}, commensurate with the increase in viscosity. We now explore the efficacy of this strategy: there is cause for optimism, since we have previously noted that observation at longer times following a potential step yields interpretable data [47].

3.2. Deposition of Ag from aqueous medium

Interpretation of the Ag and Sn data in $Ch^+Cl^-(EG)_2$ (below) will require correlation of the responses from the "E", "QCM" and "PBD" components of the experiment. We therefore need to establish some methodological and calibration capabilities in the simpler Ag/aqueous system. The first issue relates to quantitation of the QCM frequency response.

Fig. 2 shows a plot of the mass change as a function of charge passed during a cyclic voltammetric experiment commencing with a bare Au electrode onto which Ag is deposited, then stripped. The relationship is linear and shows very little hysteresis, as anticipated. The data are shown in differential form, i.e. instantaneous mass flux $\delta(\Delta m)/\delta t$ *vs* i, in Fig. 3. This presentation is intrinsically more sensitive to data quality; there is a little hysteresis, but the linearity is excellent in the deposition step (a feature that is important subsequently). A characteristic of these plots–also seen in the $Ch^+Cl^-(EG)_2$ data shown in subsequent sections - is "closure", i.e. a return to the initial state at the end of the cycle. This indicates both restoration of a clean surface at the end of the experiment and the absence of drift (whether for thermal or other reasons). Whether considered in integral or differential form, the slope of the mass *vs* charge response is within 5% of that expected on the basis of Faraday's law. These attributes collectively give confidence in the quality of the data and the facility to interpret it quantitatively in the following sections.

3.3. Deposition of Ag from $Ch^+Cl^-(EG)_2$

Having identified the origin of the experimental problem and proposed a solution, we now implement the latter. Fig. 4 shows current and optical responses during the deposition and dissolution of elemental silver from $Ch^+Cl^-(EG)_2$ at slow scan rate (ν = 0.0625 mV s^{-1}; panel *a*) and moderate scan rate (ν = 5 mV s^{-1}; panel *b*). We overlay the current and optical responses (at a given scan rate) in order to compare the fluxes at the interface and in the zone of the probe beam. At this point we focus on the two differential (flux) signals, i and θ, for which the presentational format of Fig. 4 shows that the main distinction between the data sets at different scan rates is that the optical response bears far greater similarity to the current response at slow scan rate. This is a consequence of the lesser impact of detection "at a distance" on longer timescales.

Turning to the gravimetric responses, the overall result is that on the longer timescale of the slow scan rate experiment more Ag^0 is deposited. The total Δm (not shown) is ca. 12.5 μg at ν = 0.0625 mV s^{-1} *cf.* 1.5 μg at ν = 5 mV s^{-1}. The ratio of these two, a factor of 8.3, is numerically similar to the square root of the ratio of the scan rates (a factor of 8.9), consistent with a diffusion controlled process. Since the coulometric and optical responses are obtained in differential form, it is interesting to consider the gravimetric response in this form also. As examples, Fig. 5 shows plots of the mass flux, $\delta(\Delta m)/\delta t$, *vs* charge flux, i, at the two scan rates. During deposition the plots show excellent linearity, but there is some curvature during dissolution, most noticeably at the higher scan rate; they also show "closure", i.e. return to the initial state. The slopes of the deposition half-cycle of these plots (see Table 1) are consistent with Faraday's law.

Table 1
Summary of mass change-charge relationships for Ag deposition from aq. $HClO_4$ and $Ch^+Cl^-(EG)_2$ and Sn deposition from $Ch^+Cl^-(EG)_2$.

System	Medium	ν/mV s^{-1}	Current efficiency	$S = 10^4$ d{δ(Δm)/δt}/di]/g C^{-1} [a]	$S(nF/M_W)$ [b]
Ag	aq. $HClO_4$	5	0.94	9.95	0.95
	$Ch^+Cl^-(EG)_2$	5	0.73	8.05	0.98
		0.0625	0.79	9.35	1.06
Sn	$Ch^+Cl^-(EG)_2$	0.25	≈ 1	7.37	1.25
		0.03125	0.96	8.22	1.40

[a] Measured slope of mass flux vs current plot.
[b] Ratio (dimensionless) of moles of metal atoms deposited to moles of electrons passed.

Having demonstrated how to acquire meaningful data for each component of the full EQCM/PBD experiment, we continue to focus in more detail on the more challenging PBD aspect of the experiment. Fig. 6 shows the optical response as a function of potential scan rate. While the peak current for Ag(I) reduction increases with the square root of scan rate, as one would expect for a diffusionally controlled interfacial process, the flux of species detected optically (see Eq. (1), relating θ to concentration gradient) is not even monotonic with potential scan rate. At low scan rates ($\nu \leq 0.25$ mV s^{-1}), the deflection increases with scan rate, analogous to the current data. Within this timescale regime, the optically detected flux (of silver species) is a reasonable measure of the interfacial flux (of electrons). As the scan rate is increased beyond this point ($\nu \sim 0.5$ mV s^{-1}), there is virtually no increase in optically detected flux, since the consequences of the additional consumption of Ag(I) species are not diffusionally transmitted to the laser detection zone. Further increase in scan rate ($\nu \geq 5$ mV s^{-1}) accentuates this feature, since the experimental timescale is then shorter than the transit time from surface to detector and little or nothing is detected (as discussed above).

The data of Fig. 6 provide a rational means of selecting PBD data to which the convolution process may be applied to obtain quantifiable flux data. Representative data for a slow scan rate experiment and one at the modest scan rate limit (see above) are shown in Fig. 7. The relatively good agreement on the longer timescale between the convolved interfacial responses (i and Δm) and the observed optical response (θ) is satisfying; the relatively poorer agreement on the shorter timescale is consistent with the transport limitations discussed above.

In principle, silver deposition/dissolution was selected as a mechanistically simple process to permit exploration of the chemical features of the medium and the associated instrumental capabilities. However, there is a more subtle feature of the response to silver dissolution that is revealed by the optical response, namely a double peak in the anodic θ-E signatures (see Fig. 4a). This is not seen in the i-E response or the intrinsically less sensitive integral Δm-E response. We attribute this to aspects of silver coordination chemistry in the high chloride concentration $Ch^+Cl^-(EG)_2$ medium. It is well known that silver forms anionic chloride complexes and XAS studies [48] suggest a coordination number that is between 2 and 3, i.e. formation of $[AgCl_2]^-$ and/or $[AgCl_3]^{2-}$. We argue that both species are involved at different points, as follows.

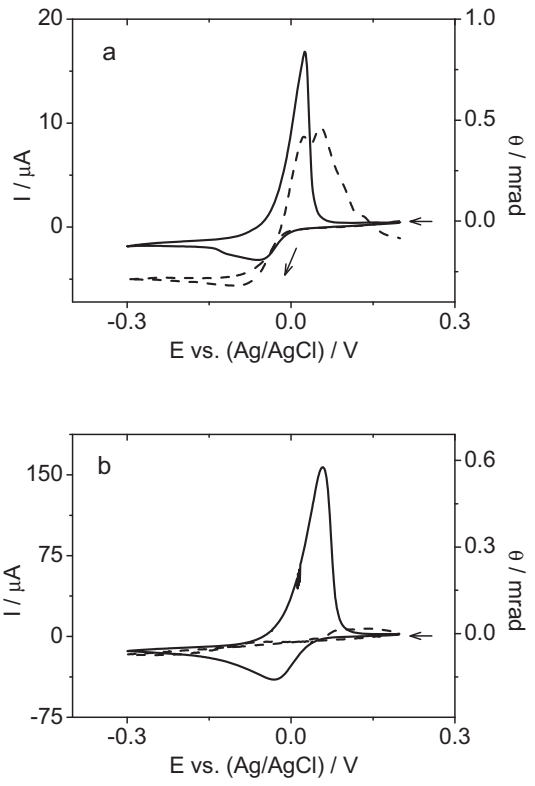

Fig. 4. Deposition of Ag from 0.01 M AgCl/$Ch^+Cl^-(EG)_2$. i-E (full lines) and θ-E (dashed lines) responses at scan rates $\nu = 0.0625$ mV s^{-1} (panel a) and $\nu = 5$ mV s^{-1} (panel b). Potential range 0.2 to -0.3 V; scan initiated from $E = 0.20$ V.

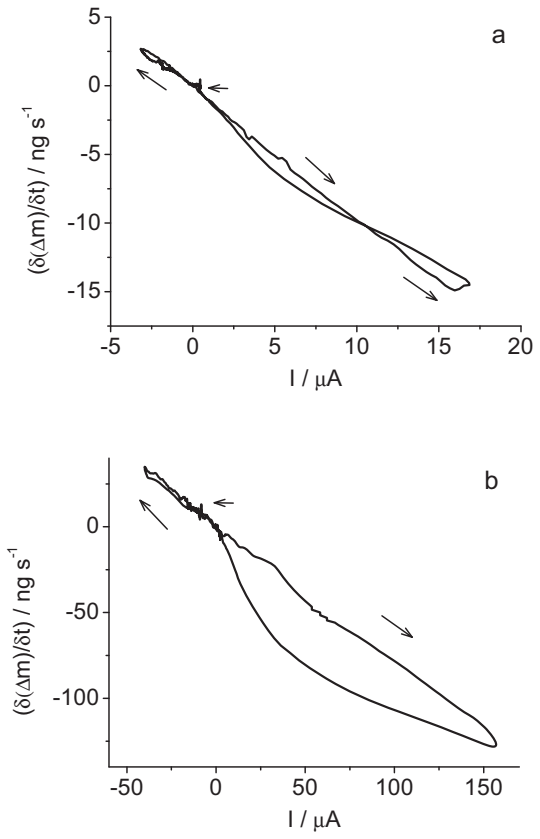

Fig. 5. Deposition of Ag from 0.01 M AgCl/$Ch^+Cl^-(EG)_2$ (the experiment of Fig. 4). Correlation of gravimetric and coulometric responses in differential form: $\delta(\Delta m)/\delta t$ vs i. Potential scan rate: $\nu = 0.0625$ mV s^{-1} (panel a) and $\nu = 5$ mV s^{-1} (panel b). Potential range 0.2 to -0.3 V; scan initiated from $E = 0.20$ V. Arrows indicate scan direction.

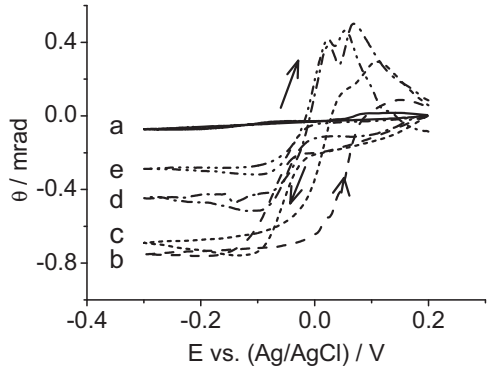

Fig. 6. Effect of potential scan rate on optical deflection (θ–E) responses during deposition of Ag from 0.01 M AgCl/Ch$^+$Cl$^-$(EG)$_2$ (the experiment of Fig. 4 and analogues at other scan rates). Potential scan rate: v/mV s^{-1} = 5 (trace *a*); 0.5 (trace *b*); 0.25 (trace *c*); 0.125 (trace *d*); 0.0625 (trace *e*), (as annotated). Potential range 0.2 to -0.3 V; scan initiated from E = 0.20 V. Arrows indicate scan direction.

As dissolution of the deposited silver commences (at $E \sim$ -0.05 V, during the anodic scan), Ag(I) species are released into a chloride-containing local environment. At this point, we note that the Ag(I) species must compete with the bidentate HBD ligands that form $[(EG)_2Cl]^-$ so, while this is a chloride-rich environment in some respects, there is not necessarily a high level of free chloride. However, as the dissolution process continues, silver ions are expelled into solution faster than the modest supply of (free) chloride is replenished by transport from the bulk of the solution. Consequently, at the outset of silver dissolution, $[AgCl_3]^{2-}$ is formed in solution but, as the concentration of solution phase Ag(I) increases

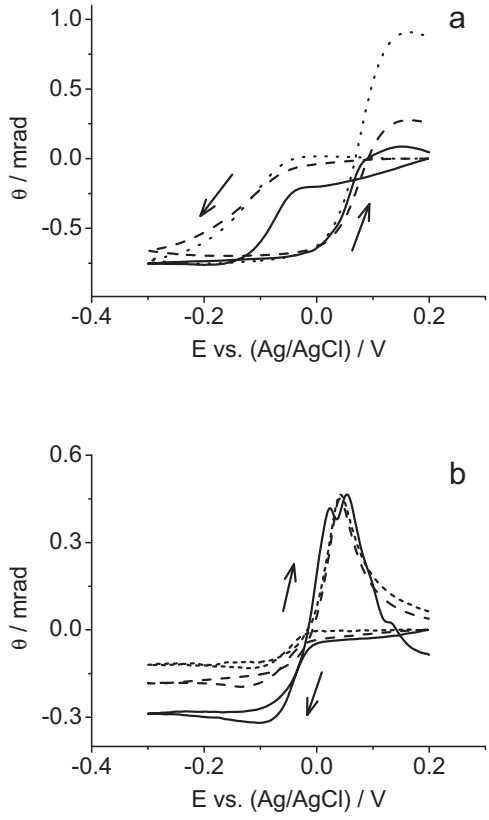

Fig. 7. Convolution of data (from Fig. 6) for deposition of Ag from 0.01 M AgCl/Ch$^+$Cl$^-$(EG)$_2$. Potential scan rate: v = 0.5 mV s^{-1} (panel a); v = 0.0625 mV s^{-1} (panel *b*). Full line: experimental θ-E response; dashed line: convolved i-E response; dotted line: convolved Δm-E response. Potential range 0.2 to -0.3 V; scan initiated from E = 0.20 V. Arrows indicate scan direction.

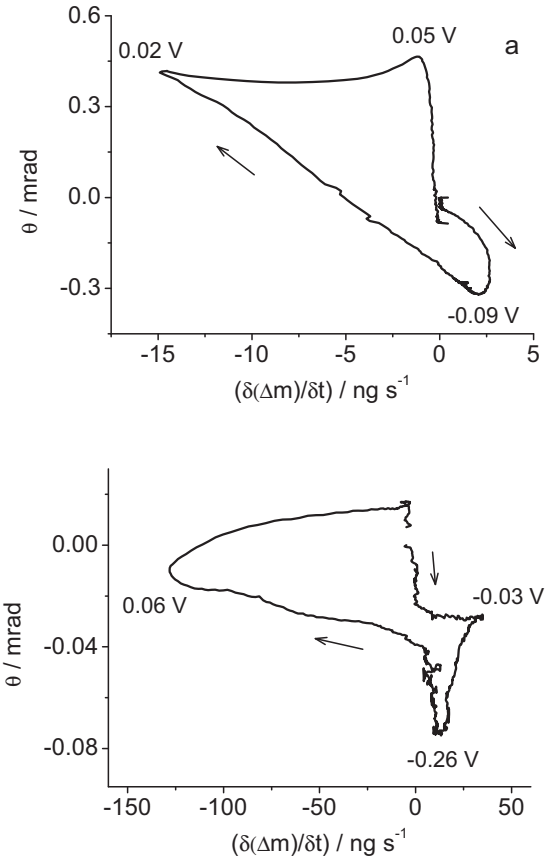

Fig. 8. Deposition of Ag from 0.01 M AgCl/Ch$^+$Cl$^-$(EG)$_2$ (the experiment of Fig. 4) Correlation of optical and gravimetric responses in differential form: θ *vs* $\delta(\Delta m)/\delta t$. Potential scan rate: v = 0.0625 mV s^{-1} (panel *a*) and v = 5 mV s^{-1} (panel *b*). Potential range 0.2 to -0.3 V; scan initiated from E = 0.20 V. Arrows indicate scan direction. Annotations indicate potentials of significant features.

and the reservoir of chloride is depleted, there is a switch to the formation of $[AgCl_2]^-$. A combination of differing redox potentials, transport rates and molar refractivities results in these two species being detected serially by the probe laser beam.

Having considered pairwise relationships between the optical and current responses and between the (differential) gravimetric and current responses, it is logical to consider the relationship between the optical and (differential) gravimetric responses. Essentially, this corresponds to viewing each of the 2D projections of the admittedly rather complicated [i, θ, $\delta(\Delta m)/\delta t$] signature. These are shown in Fig. 8 for two scan rates; given the rather novel nature of this type of plot, we attempt to make them more accessible by indicating the potentials associated with key features, i.e. turning points. We draw attention to three aspects. First, there is generally no simple relationship between the interfacial mass flux and the distant solution-positioned flux detected optically. With one exception (see below), the interfacial and solution-based gradients represented by the two responses are temporally separated, i.e. one traverses the plots in broadly horizontal or vertical stages. Second, the one exception to this is during Ag deposition at the slow scan rate, for which the timescale is such that the surface-generated concentration gradients propagate out to the probe beam and there are no complications associated with solution complexation chemistry. Third, we compare the relative magnitudes of the mass flux and optical signal excursions at the two scan rates. (Note that, in making comparisons with the analogous aqueous experiments, the silver ion concentration in the DES was deliberately chosen to be higher, to "normalize out" the effect of viscosity on reaction flux.) Inspection of the higher scan rate experiment (see Fig. 8b) shows

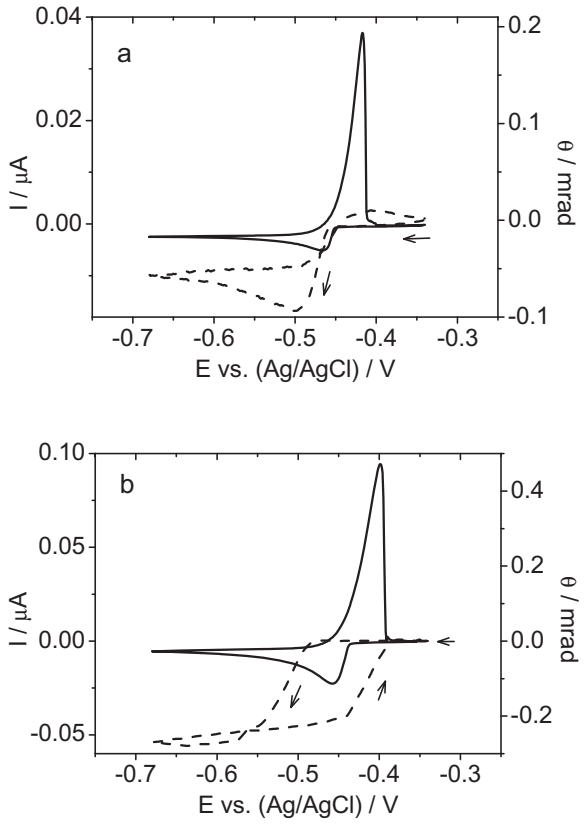

Fig. 9. Deposition of Sn from 0.01 M $SnCl_2/Ch^+Cl^-(EG)_2$. *i-E* (full lines) and θ-*E* (dashed lines) responses at scan rates $\nu = 0.03125$ mV s^{-1} (panel *a*) and $\nu = 0.25$ mV s^{-1} (panel *b*). Potential range -0.34 to -0.68 V; scan initiated from $E = -0.34$ V. Arrows indicate scan direction.

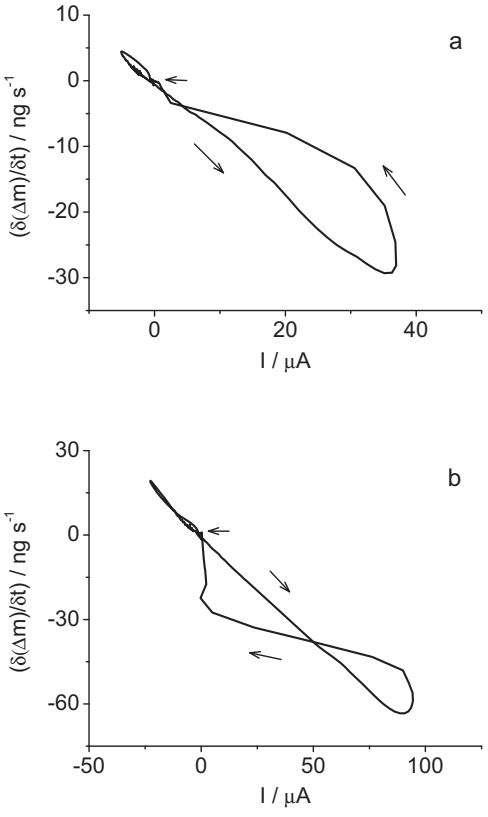

Fig. 10. Deposition of Sn from 0.01 M $SnCl_2/Ch^+Cl^-(EG)_2$ (the experiment of Fig. 9). Correlation of gravimetric and coulometric responses in differential form: $\delta(\Delta m)/\delta t$ *vs i.* Potential scan rate: $\nu = 0.03125$ mV s^{-1} (panel *a*) and $\nu = 0.25$ mV s^{-1} (panel *b*). Potential range -0.34 to -0.68 V; scan initiated from $E = -0.34$ V. Arrows indicate scan direction.

that under the conditions used the mass flux is broadly the *same* as the analogous experiment in water, while the optical signal is an order of magnitude *smaller*. Conversely, for the slower scan rate experiment, the mass flux and optical signals are *both similar* to their counterparts in water. All these are manifestations of the spatial–and thence temporal–separation of the detection systems and the key role of solution transport time in viscous media.

3.4. Deposition of Sn from $Ch^+Cl^-(EG)_2$

The unexpected facility to observe manifestations of solution chemistry of electroactive species using the PBD suggests that the technique might have wider applicability. We therefore used it to study the electrodeposition/dissolution of Sn, which is a common component of alloy coatings for surface protection, in particular as a replacement for environmentally unacceptable Cd-based systems hitherto used in physically demanding aerospace applications [49,50].

To facilitate comparisons, the presentational format of the EQCM/PBD data for these voltammetric Sn electrodeposition/dissolution experiments in $Ch^+Cl^-(EG)_2$ broadly follows that established in the preceding section for the analogous Ag experiments. Optical and current responses are superimposed in Fig. 9. Based on the experience of the Ag experiments, we used scan rates $\nu = 0.03125$ and 0.25 mV s^{-1}, which are expected to give interpretable PBD responses. The surprising outcome is that, while the current and mass (not shown in integral form) responses are perfectly well-behaved in both the forward (cathodic) and reverse (anodic) half cycles, the optical responses are not so straightforward. *Qualitatively*, at the slower scan rate, there is essentially no delay (as represented in terms of the potential axis) between the *i*- and θ- responses during the cathodic half cycle, but a noticeable delay (as represented on the potential axis) during the anodic half cycle. At the faster scan rate (see Fig. 9b), the potential shifts are greater, i.e. the temporal delay is more obvious. This trend of increasing divergence of optical and electrochemical responses as one moves to faster scan rate and from metal deposition to stripping is arguably more apparent in the overall shapes of the responses. For example, the slow scan rate cathodic θ-*E* and *i*-*E* responses look qualitatively similar, but the faster scan rate anodic θ-*E* and *i*-*E* responses are unrecognizably different. *Quantitatively*, attempts to correlate the data using the convolution process were unsuccessful in the latter instance.

In the case of the anodic responses, issues associated with DES optical characteristics, solution transport processes and experimental timescales cannot be the origin of the problem, since these are essentially identical to those of the silver experiment (see above). Instead, we are forced to consider local conditions at the interface and their chemical impact. For the purpose of argument, we consider the slower scan rate experiment of Fig. 9a, where there is no issue of solution transport limitation. During the oxidation half cycle, ca. 20 μg (ca. 0.17 μmol) of Sn is released into the solution immediately adjacent to the electrode surface (see Fig. 9b). At the slower scan rate, this takes place over an interval of ca. 3000 s, during which the diffusion layer will extend ca. 100-200 μm from the surface, i.e. well into the laser focal zone; this is consistent with the observation of an optical response. Simplistically, we can visualize the anodically stripped tin as being injected into a rather squat cylinder of solution, whose volume is the product of the electrode area (0.22 cm^2) and the distance to the laser focal zone (the "first

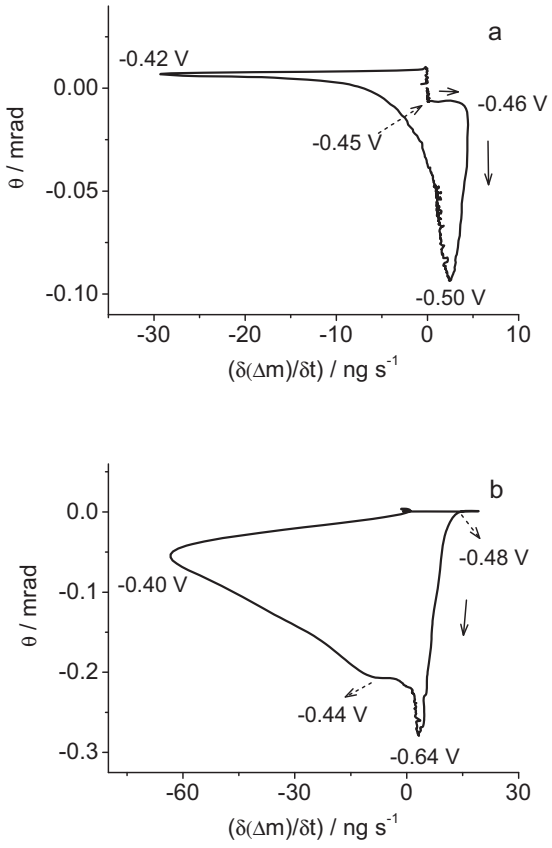

Fig. 11. Deposition of Sn from 0.01 M $SnCl_2$/$Ch^+Cl^-(EG)_2$ (the experiment of Fig. 9). Correlation of optical and gravimetric responses in differential form: θ *vs* $\delta(\Delta m)/\delta t$. Potential scan rate: $\nu = 0.0625$ mV s^{-1} (panel *a*) and $\nu = 5$ mV s^{-1} (panel *b*). Potential range -0.34 to -0.68 V; scan initiated from $E = -0.34$ V. Arrows indicate scan direction. Annotations indicate potentials of significant features.

detection point") from the electrode surface (ca. 50 μm), i.e. ca. 1 μl. This situation corresponds to an *average* Sn species concentration of ca. 0.17 mol dm^{-3}, which is approaching the solubility of $SnCl_2$ (0.2 mol dm^{-3}) in $Ch^+Cl^-(EG)_2$. Further, the nature of the diffusional process means that the *local* concentration of $SnCl_2$ will be substantially higher nearer the surface.

The corresponding mass flux *vs* current plots are shown in Fig. 10. The deposition half cycle responses are linear, although the slopes (see Table 1) suggest that there are issues associated with current efficiency under transient conditions. In contrast, the responses during the anodic (dissolution) half cycle are highly non-linear and of a scan rate dependent shape. Given the complications of solution chemistry deduced above, we speculate that a combination of density and viscosity gradients result in the liquid phase contribution to the QCM frequency response *not* being constant. As a result, for this particular instance–even though the residual film is rigid–the frequency change is not solely attributable to the surface population and the Sauerbrey equation is not applicable.

In the light of the above complications, it is unsurprising that the optical and piezoelectric responses (see Fig. 11) are not simply related. Qualitatively, their form is reminiscent of the analogous plots for the Ag system (see Fig. 8), suggesting that the broad separation of interfacial (notionally gravimetric) and solution (optical) processes still pertains, but this separation is not as straightforward.

To summarize, during the dissolution half cycle, $SnCl_2$ precipitates from the solution, resulting in a lack of soluble Sn species reaching the PBD zone on the one hand and likely scattering of light by particulates on the other hand. The end result is a PBD response that will not conform to the physical situation envisaged in the convolution process. While this might not be helpful in the sense that the probe beam does not provide additional information in the conventional sense, it has the more fundamental role of alerting us to a process of practical significance that is not immediately apparent from the *i-E* or Δm-*E* responses. The diagnostic value of the novel θ *vs* $[\delta(\Delta m)/\delta t]$ plots as a function of timescale (potential scan rate) then becomes apparent.

4. Discussion and significance

The power of the EQCM and PBD techniques to provide population changes of electroactive, exchanged or adsorbed species at the electrode/solution interface is widely appreciated and has been amply demonstrated for electrodes exposed to conventional electrolytes based on molecular solvents. General extension of this capability to other media is clearly desirable. In the case of deep eutectic solvents, both techniques are challenged by the high viscosities typical of such media. In the case of the QCM, this results in substantial energy dissipation ("damping"), in many cases to the extent that the resonator does not oscillate freely but must be driven. Fortunately, both the practicalities of this situation and the interpretation of the resulting data (analysis of the acoustic admittance curves) are well established through prior studies of viscoelastic polymer films [1–3].

However, the consequences for the PBD technique have not previously been addressed in detail. Here, the limiting factor is associated with the transit time of interfacially generated/consumed species between the electrode and the focal zone of the probe beam. Under typical instrumental conditions, this transit time is a few seconds through fluids with viscosities similar to water but may be hundreds of seconds for ionic liquids (exemplified here by in $Ch^+Cl^-(EG)_2$. The result is that essentially no compositional change is detected optically on the timescale of a typical voltammetric experiment.

The most obvious strategy to overcome this problem is to decrease the distance (and thence transit time) between the surface and the laser focal zone. This is only practical to a limited extent, since the distance is only about 2-3 times the diameter of the laser focal zone. If the edge of the beam impinges on the electrode, then light scattering will become a problem. Tightening the focus is not an option, since this would only be in a limited part of the path across the face of the electrode; the divergence of the beam in other regions would be increased.

The successful strategy demonstrated here involves extension of the experimental timescale to permit the interfacially generated/consumed species adequate time to diffuse to/from the laser focal zone. In a voltammetric experiment, this is implemented by decreasing the potential scan rate. Two practical consequences of increasing the timescale are the need for effective temperature control and consideration of possible convective enhancement of solution mass transport. These two are to some extent linked, since inadequate temperature control will not only generate refractive index gradients directly but will also create density gradients that lead to convection. While the convection issue initially seems problematical, the routine mounting of the instrumentation on an optical table is designed to minimise vibration. Further, the viscosity effects that necessitate the use of extended timescales also extend the timescale associated with convection. Thus, in practice, the problem is manageable.

The $Ag^{+/0}$ system has frequently been used for calibration of electrogravimetric methodologies–with its origins in the classical experiments of Faraday–but in the DES medium used here there is the interesting addition of speciation effects due to chloride

complexation. These are manifested during the anodic (stripping) half of the cycle, when substantial amounts of Ag(I) are injected into the solution and the Ag(I):Cl^- ratio varies significantly. The $Sn^{2+/0}$ redox system also involves chloride complex formation, but here the complication arises as a consequence of locally exceeding the solubility limit when tin ions are released into a relatively small volume of solution between the electrode surface and the probe beam.

Consideration of the correlations between the various flux parameters (i, $\delta(\Delta m)/\delta t$ and θ) turns out to be of general diagnostic value and, in simpler cases, amenable to quantitative interpretation via the convolution operation. The general feature here is that the E and QCM components of the EQCM/PBD experiment provide responses (i and Δm) during the dissolution process that are *not* influenced by solution chemistry, while the PBD component of the experiment provides a response (θ) that *is* sensitive to solution chemistry. The former provide simplicity and the latter provides insight, albeit at the cost of some interpretational effort. This combination suggests that the combined methodology will be useful for studying coupled electrochemical/chemical (so-called "EC"-type) processes that may be expected to be extremely common for metal species in DES and similar media such as ionic liquids.

5. Conclusions

We have demonstrated that the combined EQCM/PBD technique can be used to study (electro)chemical processes in ionic liquids, such as deep eutectic solvents (here, represented by in $Ch^+Cl^-(EG)_2$. From the perspective of the PBD part of the measurement, which has not been previously reported for such media, the critical issue is the long transit time of species through the very viscous solution between the electrode surface and the probe beam. A simple strategy for dealing with this in the context of a voltammetric experiment is to move to slower scan rates, typically by one or two orders of magnitude compared to the analogous experiment in a simple molecular solvent.

The use of the $Ag^{+/0}$ redox system as a validation or calibration system, as commonly done for molecular solvent-based electrolytes, works perfectly well during elemental silver deposition from in $Ch^+Cl^-(EG)_2$. However, during the reverse (anodic stripping) process, the complexation chemistry of silver becomes apparent. As the local availability of free chloride ion is challenged by increasing concentrations of silver ion, there is evidence for the interplay of $[AgCl_3]^{2-}$ and $[AgCl_2]^-$ species. The $Sn^{2+/0}$ system also involves chloride complex formation, but here the complication arises as a consequence of locally exceeding the solubility limit when tin ions are released into a relatively small volume of solution between the electrode surface and the probe beam.

We conclude that the component responses of the EQCM/PBD experiment are in fact even more complementary than commonly recognized. In additional to their individual merits as measured, consideration of the time differential of the mass (the mass flux) not only provides a calibration (essentially, an instantaneous implementation of Faraday's law) but also makes the gravimetric signal directly comparable with the coulometric and optical signals. Correlations between the various flux parameters (i, $\delta(\Delta m)/\delta t$ and θ) have general diagnostic value and, in simpler cases, amenable to quantitative interpretation via the convolution operation.

That the electrochemical, gravimetric and optical responses are sensitive, respectively, to electroactive (only), heavy (preferentially, but irrespective of charge) and electrolyte contrasted (optically distinct) species is generally appreciated. However, the additional feature that emerges is the distinction between responses (i and Δm) during the dissolution process that are *not* influenced by solution chemistry and that (θ) which *is*. We suggest that this attribute might be more widely exploited in the study of coupled electrochemical/chemical ("EC"-type) processes.

Acknowledgements

V.C. Ferreira and C.J. Zaleski grateful acknowledge the financial support from Fundação para a Ciência e a Tecnologia, scholarship SFRH/BPD/77404/2011 and European Commission, FP7 project POLYZION (FP7-ENERGY-NMP-2008-1 226655, http://www.polyzion.eu).

References

[1] A.R. Hillman, The electrochemical quartz crystal microbalance, in Encyclopaedia of Electrochemistry, A.J., Bard, M. Stratmann (Eds.), Wiley, New York, vol. 3, pp. 230-289.
[2] D. Johannsmann, Viscoelastic, mechanical, and dielectric measurements on complex samples with the quartz crystal microbalance, Phys. Chem. Chem. Phys 10 (2008) 4516–4534.
[3] A.R. Hillman, The EQCM: electrogravimetry with a light touch, J. Solid State Electrochem. 15 (2011) 1647–1660.
[4] C. Barbero, M.C. Miras, R. Kotz, O. Haas, Probe beam deflection - a useful tool for the study of ion transport in polymers, Solid State Ionics 60 (1993) 167–172.
[5] C.A. Barbero, Ion exchange at the electrode/electrolyte interface studied by probe beam deflection techniques, Phys. Chem. Chem. Phys. 9 (2005) 1885–1899.
[6] G.G. Láng, C.A. Barbero, Laser Techniques for the Study of Electrode Processes, Springer-Verlag, Berlin, 2012.
[7] S. Servagent, E. Vieil, In-situ quartz microbalance study of the electrosynthesis of poly(3-methylthiophene), J. Electroanal. Chem. 280 (1990) 227–232.
[8] N. Lassalle, A. Roget, T. Livache, P. Mailley, E. Vieil, Electropolymerisable pyrrole- oligonucleotide: synthesis and analysis of ODN hybridisation by fluorescence and QCM, Talanta 55 (2001) 993–1004.
[9] O. Schneider, A. Bund, A. Ispas, N. Borissenko, S.Z. El Abedin, F. Endres, EQCM study of the electropolymerization of benzene in an ionic liquid and ion exchange characteristics of the resulting polymer film, J. Phys. Chem. B 109 (2005) 7159–7168.
[10] M.A. Mohamoud, A.R. Hillman, Viscoelastic phenomena during electrochemical deposition of polyaniline films, J. Sol. State Electrochem. 11 (2007) 1043–1050.
[11] M. Skompska, A. Tarajko-Wazny, EQCM studies of polymerization and redox process of poly(1,8-diaminocarbazole) in protic and aprotic solutions, Electrochim Acta 56 (2011) 3494–3499.
[12] H. Gomez, R. Henriquez, R. Schrebler, G. Riveros, R. Cordova, Nucleation and growth mechanism of CdTe at polycrystalline gold surface analysed through (m-t simulation transient, Electrochim. Acta 46 (2001) 821–827.
[13] Z. Jusys, H. Massong, H. Baltruschat, A new approach for simultaneous DEMS and EQCM: electrooxidation of adsorbed CO on Pt and Pt-Ru, J. Electrochem. Soc. 146 (1999) 1093–1098.
[14] P. Kern, D. Landolt, Adsorption of organic corrosion inhibitors on iron in the active and passive state. A replacement reaction between inhibitor and water studied with the rotating quartz crystal microbalance, Electrochim. Acta 47 (2001) 589–598.
[15] A. Glidle, A.R. Hillman, K.S. Ryder, E.L. Smith, J.M. Cooper, R. Dalgliesh, R. Cubitt, T. Geue, Metal chelation and spatial profiling of components in crown ether functionalised conducting polymer films, Electrochim. Acta 55 (2009) 439–450.
[16] M. Hepel, S. Bruckenstein, K. Kanige, Expulsion of borate ions from the silver solution interfacial region during underpotential deposition discharge of Bi(III) in borate buffer, Far. Trans. 89 (1993) 251–254.
[17] M.C. Santos, M.F. Cabral, S.A.S. Machado, Tellurium underpotential deposited ad-atoms on Au electrodes: a new electrodeposition mechanism using an electrochemical quartz crystal nanobalance, Electrochim. Acta 58 (2011) 1–5.
[18] A.R. Hillman, D.C. Loveday, S. Bruckenstein, Thermodynamic changes in ion and solvent populations accompanying redox switching in polyvinylferrocene films, J. Electroanal. Chem. 274 (1989) 157–166.
[19] A.R. Hillman, M.J. Swann, S. Bruckenstein, Ion and solvent transfer accompanying polybithiophene doping and undoping, J. Electroanal. Chem. 291 (1990) 147–162.
[20] E. Vieil, K. Meerholz, T. Matencio, J. Heinze, Mass transfer and convolution: part II in situ optical beam deflection study of ionic exchange between polyphenylene films and a 1:1 electrolyte, J. Electroanal. Chem. 368 (1994) 183–191.
[21] J. Bacskai, K. Martinusz, E. Czirok, G. Inzelt, M.A. Malik, P.J. Kulesza, Polynuclear nickel hexacyanoferrates–monitoring of film growth and hydrated countercation flux storage during redox reactions, J. Electroanal. Chem. 385 (1995) 241–248.
[22] A. Bund, S. Neudeck, Effect of the solvent and the anion on the doping/dedoping behaviour of poly(3,4-ethylenedioxythiophene) films studied with the electrochemical quartz microbalance, J, Phys. Chem. B 108 (2004) 17845–17850.
[23] A.R. Hillman, S.J. Daisley, S. Bruckenstein, Kinetics and mechanism of the electrochemical p-doping of PEDOT, Electrochem. Commun. 9 (2007) 1316–1322.
[24] L.T.T. Kim, C. Gabrielli, H. Perrot, J. Garcia-Jareno, F. Vicente, Redox switching of Prussian Blue films investigated by ac-electrogravimetry, Electrochim. Acta 84 (2012) 35–48.

[25] H.J. Salavagione, J. Arias-Pardilla, J.M. Perez, J.L. Vazquez, E. Morallon, M.C. Miras, C. Barbero, Study of redox mechanism of poly(o-aminophenol) using in situ techniques: evidence of two redox processes, J. Electroanal. Chem. 576 (2005) 139–145.
[26] A.R. Hillman, M.A. Mohamoud, Ion, solvent and polymer dynamics in polyaniline conducting polymer films, Electrochim. Acta 51 (2006) 6018–6024.
[27] C.A. Barbero, M.C. Miras, O. Haas, R. Kotz, Direct in situ evidence for proton anion exchange in polyaniline films by means of probe beam deflection, J. Electrochem. Soc. 138 (1991) 669–672.
[28] L.M. Abrantes, J.P. Correia, On the initiation and growth of polymer films onto electrode surfaces, Electrochim. Acta 44 (1999) 1901–1910.
[29] J.P. Correia, E. Vieil, L.M. Abrantes, Electropolymerization of 3-methylthiophene studied by multiflux convolution, J. Electroanal. Chem. 573 (2004) 299–306.
[30] M.J. Henderson, E. Bitziou, A.R. Hillman, E. Vieil, Lead underpotential deposition on polycrystalline gold electrode in perchloric acid solution: a combined electrochemical quartz crystal microbalance (EQCM) and probe beam deflection (PBD) study, J. Electrochem. Soc. 148 (2001) E105–E111.
[31] M.J. Henderson, A.R. Hillman, E. Vieil, C. Lopez, Combined electrochemical quartz crystal microbalance (EQCM) and probe beam deflection (PBD): validation of the technique by a study of silver ion mass transport, J. Electroanal. Chem. 458 (1998) 241–248.
[32] M.J. Henderson, A.R. Hillman, Ion and solvent transfer discrimination at a poly(o-toluidine) film exposed to $HClO_4$ by combined EQCM and PBD, J. Phys. Chem. B 103 (1999) 8899–8907.
[33] A.P. Abbott, K.J. McKenzie, Application of ionic liquids to the electrodeposition of metals, Phys. Chem. Chem. Phys. 8 (2005) 4265–4279.
[34] A.P. Abbott, D. Boothby, G. Capper, D.L. Davies, R.K. Rasheed, Deep eutectic solvents formed between choline chloride and carboxylic acids: versatile alternatives to ionic liquids, J. Am. Chem. Soc. 126 (2004) 9142–9147.
[35] Q. Zhang, K. De Oliviera Vigier, S. Royer, F. Jérôme, Deep eutectic solvents: syntheses, properties and applications, Chem. Soc. Rev. 41 (2012) 7108–7146.
[36] A.P. Abbott, G. Frisch, K.S. Ryder, Electroplating Using Ionic Liquids, Annu. Rev. Mater. Res. 43 (2013) 335–358.
[37] E.M. Moustafa, S.Z. El Abedin, A. Shkurankov, E. Zschippang, A.Y. Saad, A. Bund, F. Endres, Electrodeposition of Al in 1-butyl-1-methylpyrrolidinium bis(trifuoromethylsulfonyl)amide and 1-ethyl-3-methylimidazolium bis(trifluoromethylsulfonyl)amide ionic liquids: in situ STM and EQCM studies, J. Phys. Chem. B 111 (2007) 4693–4704.
[38] A. Ispas, M. Polleth, H.T.B. Khanh, A. Bund, J. Janek, Electrochemical deposition of silver from 1-ethyl-3-methylimidazolium trifluoromethanesulfonate, Electrochim. Acta 56 (2011) 10332–10339.
[39] N. Serizawa, N. Tachikawa, Y. Katayama, T. Miura, EQCM measurement of Sn(II)/Sn reaction in 1-butyl-1-methylpyrrolidinium bis(trifluoromethylsulfonyl)amide room-temperature ionic liquid, Electrochemistry 77 (2009) 630–632.
[40] N. Serizawa, Y. Katayama, T. Miura, EQCM measurement of Ag(I)/Ag reaction in an amide-type room-temperature ionic liquid, J. Electrochem. Soc. 156 (2009) D503–D507.
[41] A.P. Abbott, K. El Ttaib, G. Frisch, K.J. McKenzie, K.S. Ryder, Electrodeposition of copper composites from deep eutectic solvents based on choline chloride, Phys. Chem. Chem. Phys. 11 (2009) 4269–4277.
[42] M.A. Skopek, M.A. Mohamoud, K.S. Ryder, A.R. Hillman, Nanogravimetric observation of unexpected ion exchange characteristics for polypyrrole film p-doping in a deep eutectic ionic liquid, Chem Commun. 93 (2009) 5–93, 7.
[43] A.P. Abbott, S. Nandhra, S. Postlethwaite, E.L. Smith, K.S. Ryder, Electroless deposition of metallic silver from a choline chloride-based ionic liquid: a study using acoustic impedance spectroscopy, SEM and atomic force microscopy, Phys. Chem. Chem. Phys. 9 (2007) 3735.
[44] G. Sauerbrey, Vervendung von Schwingquarzen zur Wägung dünner Schichten und zur Mikrowägung, Z. Phys 155 (1959) 206–222.
[45] E. Vieil, Mass transfer and convolution. 1. Theory, J. Electroanal. Chem. 264 (1994) 9–15.
[46] R.B. Leron, A.N. Soriano, M.-H. Li, Densities and refractive indices of the deep eutectic solvents (choline chloride plus ethylene glycol or propylene glycol) and their aqueous mixtures at the temperature ranging from 298.15 K to 333.15 K, J. Taiwan Inst. Chem. Eng. 43 (2012) 551–557.
[47] A.R. Hillman, K.S., Ryder, V.C., Ferreira, C.J., Zaleski, E. Vieil, Ion transfer dynamics of poly(3,4-ethylenedioxythiophene) films in deep eutectic solvents, Electrochim. Acta, in press.
[48] A.P. Abbott, K.E. Ttaib, G. Frisch, K.S. Ryder, D. Weston, The electrodeposition of silver composites using deep eutectic solvents, Phys. Chem. Chem. Phys. 14 (2012) 2443–2449.
[49] K.R. Baldwin, C.J.E. Smith, Advances in replacements for cadmium plating in aerospace applications, Trans. Inst. Met. Finishing 74 (1996) 202–209.
[50] F. Gao, R. Liu, X.J. Wu, Tribaloy alloy reinforced tin-bronze composite coating for journal bearing applications, Thin Solid Films 519 (2011) 4809–4817.